

Catalytic hairpin assembly gel assay for multiple and sensitive microRNA detection

Wenhao Dai¹, Jing Zhang², Xiangdan Meng¹, Jie He³, Kai Zhang¹, Yu Cao¹, Dongdong Wang¹, Haifeng Dong^{1,*}, Xueji Zhang^{1,*}

1. Research Center for Bioengineering and Sensing Technology, Beijing Key Lab for Bioengineering and Sensing Technology, School of Chemistry and bioengineering, University of Science & Technology Beijing, Beijing 100083, P.R. China.
2. School of Petrochemical Engineering, School of Food Science and Technology, Changzhou University, Changzhou 213164, P.R. China.
3. School of Computer and Communication Engineering, University of Science & Technology Beijing, Beijing 100083, P.R. China.

Corresponding author: hfdong@ustb.edu.cn; zhangxueji@ustb.edu.cn.

Phone/Fax: +86 010 82376576.

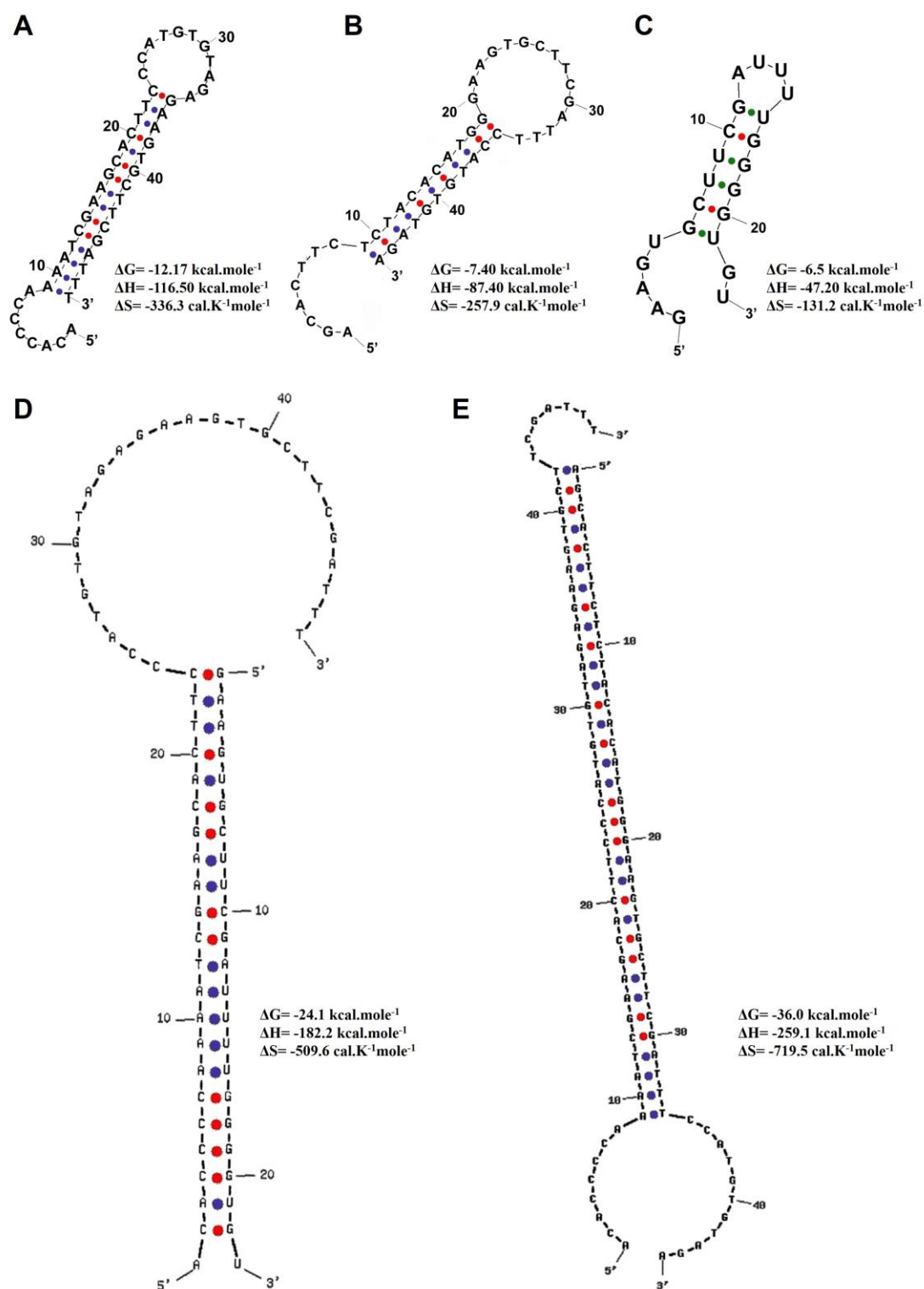


Figure S1. (A) Ideal structure and thermal kinetic parameters of HDP-373, (B) HAP-373, (C) miRNA-373, (D) HDP-miRNA-373 duplex and (E) HDP/HAP-373 complexes.

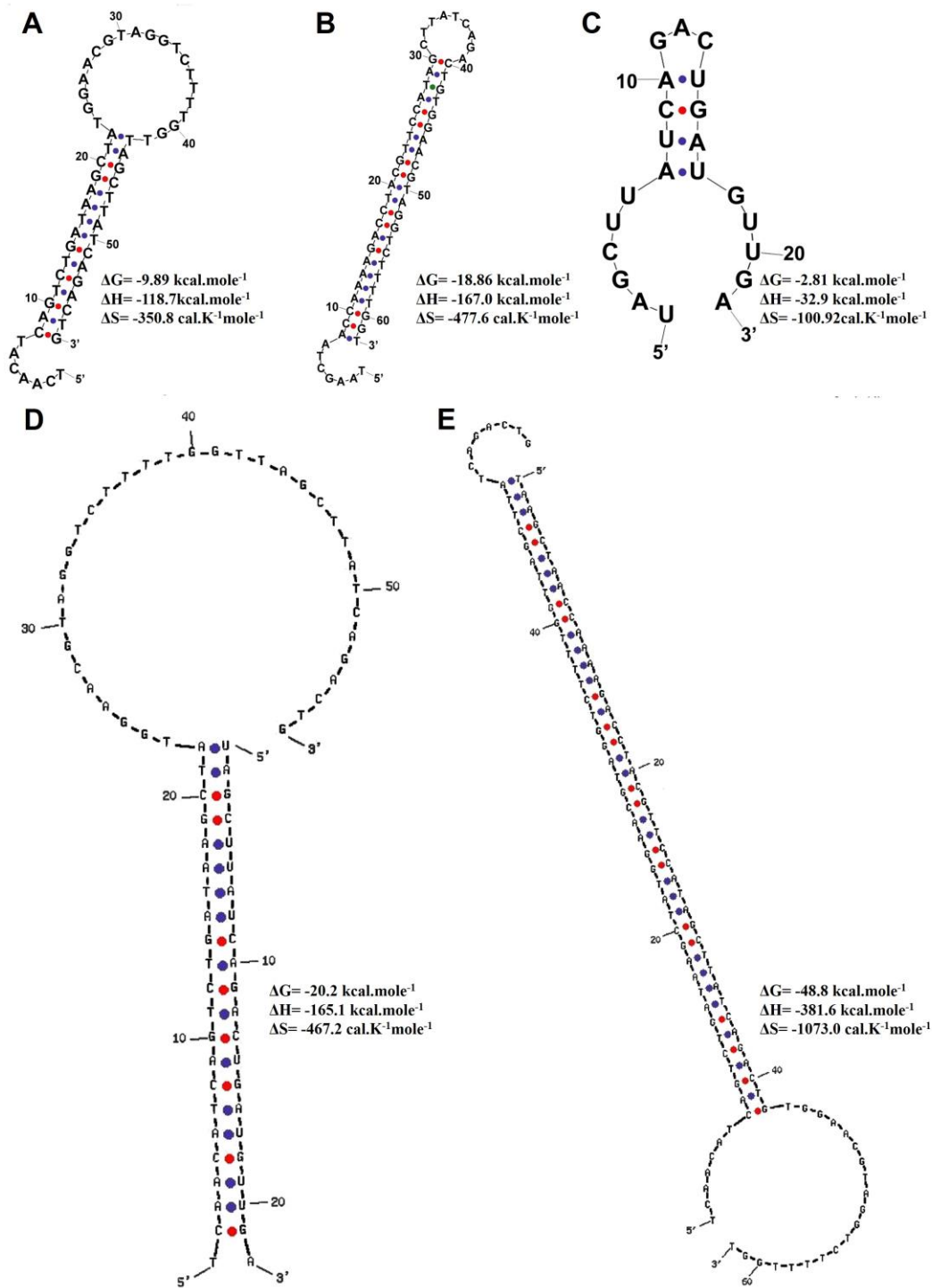


Figure S2. (A) Ideal structure and thermal kinetic parameters of HDP-21, (B) HAP-21, (C) miRNA-21, (D) HDP-miRNA-21 duplex and (E) HDP/HAP-21 complexes.

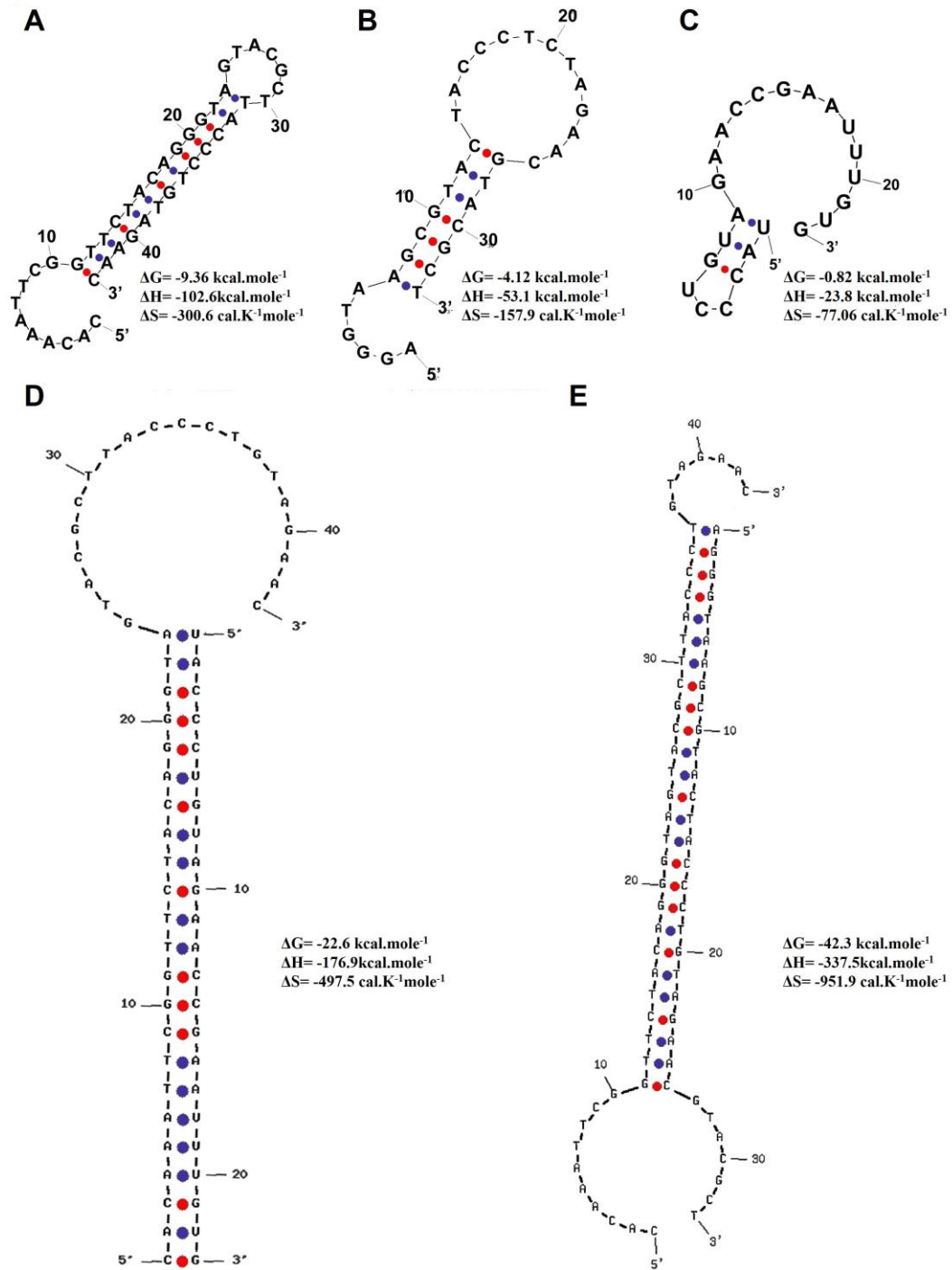


Figure S3. (A) Ideal structure and thermal kinetic parameters of HDP-10b, (B) HAP-10b, (C) miRNA-10b, (D) HDP-miRNA-10b duplex and (E) HDP/HAP-10b complexes.

Characterization of CHA kinetics

The CHA kinetics were determined using the 'fminunc' function in Matlab. 100 nM HDP with two terminals labeled with a fluorescent dye and quencher, 100 nM HAP, and target miRNA-21 and miRNA-10b with different concentrations were mixed, and the fluorescent intensity of the solution was detected as a function of time.

In order to convince the progress of CHA reaction, time course of the CHA reaction over a wide range of target miRNA concentrations was produced by fluorescent spectra (Figure S4). The kinetic analysis of the CHA was carried out using the 'fminunc' function in Matlab. The rate constant $k_{all} = 0.9 \times 10^5 \text{ M}^{-1}\text{s}^{-1}$ of miRNA-21 yielded the best fit to the experimental data in Figure S4A, and the $k_{all} = 4.5 \times 10^5 \text{ M}^{-1}\text{s}^{-1}$ of miRNA-10b is plotted as dots in Figure S4B. The displaced length of HAP of miRNA-10b is shorter than that of miRNA-21, resulting in the rate constant of miRNA-10b is five times higher than miRNA-21. Therefore, It kinetically suggested the good feasibility of the CHA process.

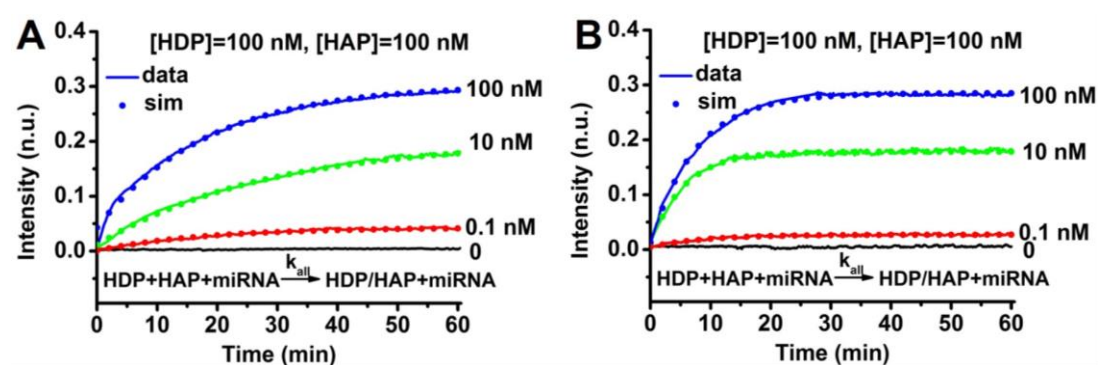


Figure S4. Characterization of CHA kinetics. (A) Measurement catalyst binding rate k_{all} of miRNA-21. All traces contain 100 nM HDP, 100 nM HAP initially, and different amounts of target miRNA-21 were added at $t \approx 0$. Dotted lines show simulation traces modelling reactions, assuming rate constant $k_{all} = 0.9 \times 10^5 \text{ M}^{-1}\text{s}^{-1}$. (B) Measurement catalyst binding rate k_{all} of miRNA-10b. All traces contain 100 nM HDP, 100 nM HAP initially, and different amounts of target miRNA-10b were added at $t \approx 0$. Dotted lines show simulation traces modelling reactions, assuming rate constant $k_{all} = 4.5 \times 10^5 \text{ M}^{-1}\text{s}^{-1}$. "n.u." denotes normalized units; all fluorescent results were normalized so that 1 n.u.

Experimental Conditions Optimization

To optimize the ratio of HDP:HAP, HDP (1 μ M) was mixed with different concentration of HAP (0.25, 0.5, 1, 2, 4 μ M) and target miRNA-373 (100 nM) in 50 μ L hybridization buffer for 1 h at 37 $^{\circ}$ C. 5 μ L of the resulting mixture was mixed with 1 μ L (6 \times loading buffer) and analyzed by gel electrophoresis (4.0 % agarose gel) using 1 \times TAE buffer as the running buffer and run for 1 h at a 100 mA. The gel images were acquired with a gel-imaging system with 40 ms exposure time.

For optimizing the reaction time, HDP (1 μ M) was mixed with HAP (1 μ M) and target miRNA-373 (100 nM) in 50 μ L hybridization buffer, reacting at 37 $^{\circ}$ C for different time (20, 40, 60, 80, 100, 120 min). 5 μ L of the resulting mixture was mixed with 1 μ L (6 \times loading buffer) and analyzed by gel electrophoresis as the process aforementioned. The reaction temperature was optimized as follows: HDP (1 μ M) was mixed with HAP (1 μ M) and target miRNA-373 (100 nM) in 50 μ L hybridization buffer, reacting at different temperature (4, 20, 32, 37, 42, 45, 55 $^{\circ}$ C) for 1 h. The resulting mixture was analyzed by gel electrophoresis in a similar process aforementioned.

In order to achieve ideal analytical performance, different experimental conditions have been optimized. We firstly investigated the optimized HDP:HAP ratio. As shown in **Figure S5A**, the gel band intensity related to the HDP/HAP complexes sharply increased along with the increase of the HDP:HAP ratio from 1:0.25 to 1:1 and the gel band intensity further slightly increased when the HDP:HAP ratio increased from 1:1 to 1:2. The gel intensity was normalized by the lowest gel intensity presented in the gel band to obtain the normalized curve (**Figure S5D**), indicating 1:1 was the optimal ratio of HDP:HAP. The incubation temperature is an important parameter of reaction kinetics that determines the probability of collisions between the molecules [1]. In CHA reaction gel assay, incubation temperature is a key factor that influences the stability and interaction of the two hairpin probes. At low incubation temperature, the two hairpins could not react effectively with the target that greatly extended the reaction time. However, with higher incubation temperature, the stability of the two hairpins would decrease, and caused the lower specificity. **Figure S5B** and **Figure S5E** (normalized by the lowest gel intensity) revealed the gel band intensity related to HDP/HAP complexes increased while the incubation temperature raised from 4 to 37 $^{\circ}$ C, and further increase of incubation temperature induced the decrease of the gel band intensity, which was resulted from the non-specific products of non-stable hairpins at high temperature. Thus, 37 $^{\circ}$ C was selected for the optimal incubating temperature. In addition, the incubation time was also examined from 20-120 min, and the maximum gel band intensity was achieved at 60 min (**Figure S5C** and **S5F**). The slight decrease of the gel band after 60 min resulted from the degradation of the miRNA and the stability of the HDP/HAP simultaneously.

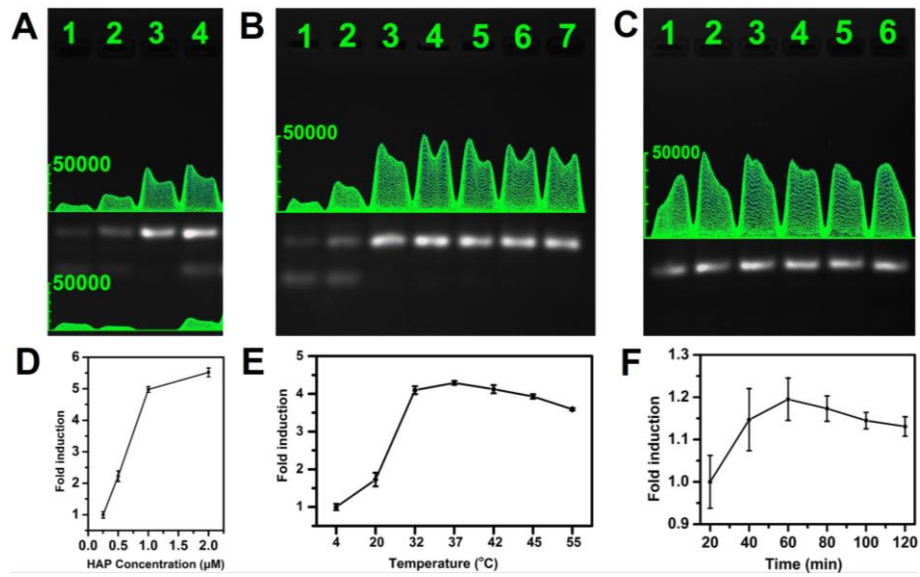


Figure S5. Optimization of (A) the ratio of HDP:HAP (HDP: 1 μM and target miRNA: 100 nM; 37 $^{\circ}\text{C}$; 60 min), (B) incubating temperature (HDP: 1 μM , HAP: 1 μM and target miRNA: 100 nM; 60 min), and (C) incubating time (HDP: 1 μM , HAP: 1 μM and target miRNA: 100 nM; 37 $^{\circ}\text{C}$). The average fold induction values for the corresponding gel band gray-value (D) the ratio of HDP:HAP, (E) incubating temperature, and (F) incubating time; which is normalized with the negative control band, and the error bars were obtained from three independent assays for each case.

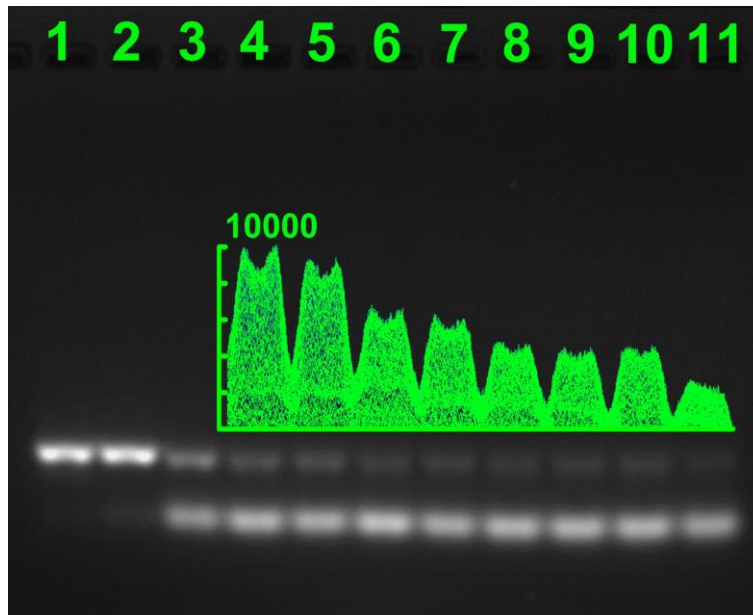


Figure S6. Sensitivity of the CHA gel assay. The CHA gel assay results to different concentration of target miRNA-373 (Lane 1-11: 1 μ M, 100 nM, 10 nM, 1 nM, 100 pM, 10 pM, 1 pM, 100 fM, 10 fM, 1 fM and 0).

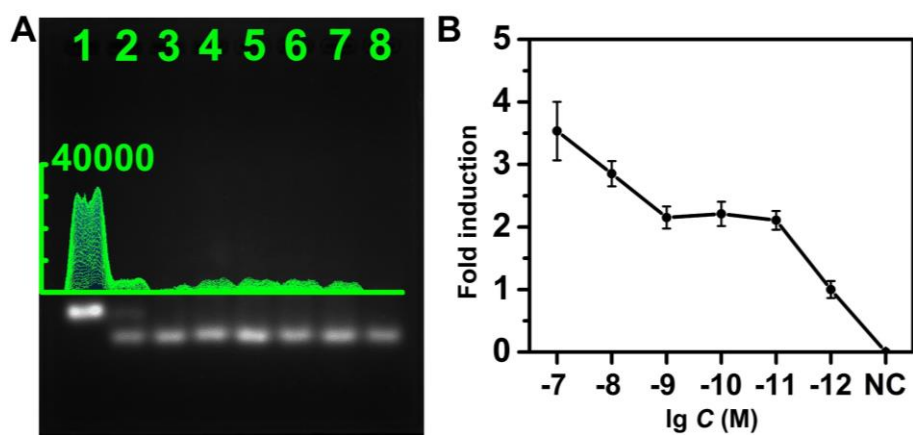


Figure S7. (A) The non-amplification gel assay results and (B) corresponding calibration curve to different concentration of target miRNA (Lane1-8: 1 μ M, 100 nM, 10 nM, 1 nM, 100 pM, 10 pM, 1 pM and 0), normalized with the 1 pM target band, and the error bars were obtained from three independent assays for each case.

Sensitivity of CHA Gel Assay

Under optimized experiment conditions. HDP (1 μM), HAP (1 μM) and different concentration of target miRNA-21 and miRNA-10b (Lane1-9: 1 μM , 100 nM, 10 nM, 1 nM, 100 pM, 10 pM, 1 pM, 100 fM and 0) in 50 μL was reacted for 1 h at 37 $^{\circ}\text{C}$. The resulting mixture was analyzed by gel electrophoresis.

As shown in **Figure S8A** and **S8B**, the HDP/HAP complexes decreased gradually with falling concentration of target miRNA-21. The correspond calibration plots showed a good linear relationship between the fold induction and the logarithm of miRNA-21 concentrations in the range from 100 fM to 1 nM (inset of **Figure S8B**), with a linear equation of $F/F_0=10.7246 + 0.7422 \lg C \text{ (M)}$ ($R^2=0.9815$). The LOD was calculated by using three times the standard deviation corresponding to the control sample detection, which was estimated as low as 25 fM. The LOD of miRNA-10b in **Figure S8C** and **S8D** was calculated to 46 fM, with a linear equation of $F/F_0=18.765+ 1.34168 \lg C \text{ (M)}$ ($R^2=0.9921$).

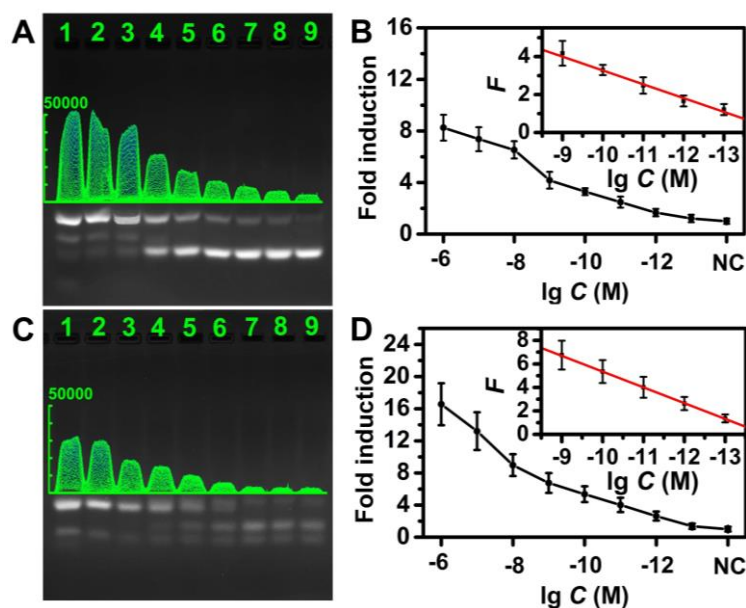


Figure S8. (A) The CHA gel assay results and (B) corresponding calibration curve to different concentration of target miRNA-21 (Lane 1-9: 1 μM , 100 nM, 10 nM, 1 nM, 100 pM, 10 pM, 1 pM, 100 fM and 0). (C) The CHA gel assay results and (D) corresponding calibration curve to different concentration of target miRNA-10b (Lane 1-9: 1 μM , 100 nM, 10 nM, 1 nM, 100 pM, 10 pM, 1 pM, 100 fM and 0). Normalized with the negative control band, and the error bars were obtained from three independent assays for each case.

Fluorescent spectrometry experiment

In order to analyze the CHA reaction mixtures by fluorescent spectrometry, we carried out an amplification assay to investigate the validity of the proposed CHA gel assay. In brief, 100 nM HDP with two terminals labeled with a fluorescent dye and a quencher was mixed with different concentrations of target miRNA-373 with 100 nM HAP. The solution were then incubated for 1 h at 37 °C. After the incubation, the solution were diluted and analyzed by fluorescent spectrometry. As shown in **Figure S7**, the fluorescence intensity increased with elevated concentration of target miRNA-373. The calibration plots showed a good linear relationship between the fluorescence intensity and the logarithm of miRNA-373 concentrations in the range from 0.1 nM to 1 μM (inset of **Figure S6**), with a linear equation of F/F_0 (au) = 6.62233 + 0.53841 lgC (M) ($R^2=0.9989$). The limit of detection (LOD) was calculated by using three times the standard deviation corresponding to the control sample detection, which was estimated as low as 38 pM. These resulting further indicated the formation of the HDP-HAP reaction mixture, and validated the CHA assay in quantitative analysis.

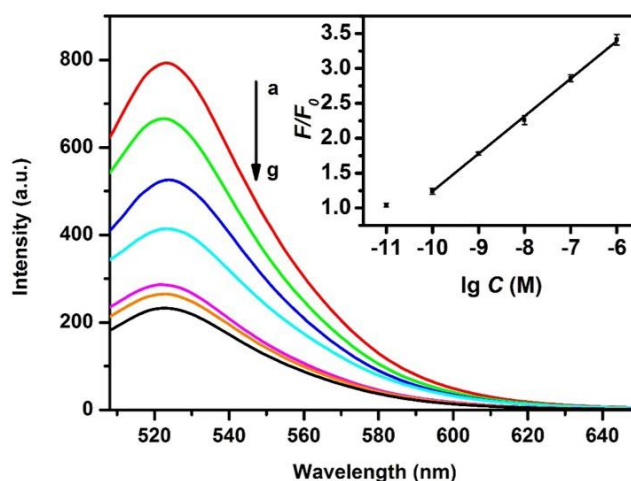


Figure S9. Typical fluorescence emission of the solution containing HDP (100 nM), HAP (100 nM) and different concentrations of target miRNA-373. From bottom to top: 0, 10 pM, 100 pM, 1 nM, 10 nM, 100 nM, 1 μM. Inset: the corresponding calibration plot of fluorescence intensity vs. lg C.

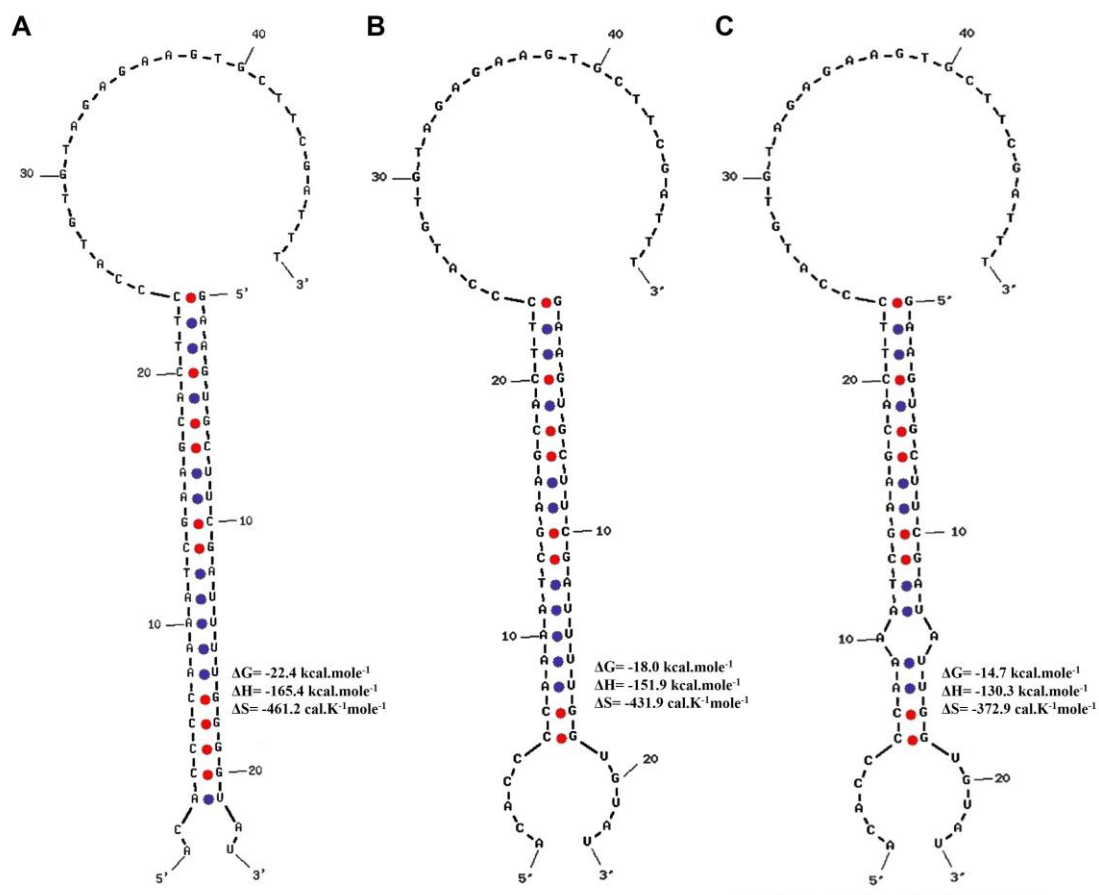


Figure S10. (A) Ideal structure and thermal kinetic parameters of HDP/SM complexes, (B) HDP/DM complexes and (C) HDP/TM complexes.

Table S1. Comparison of different CHAs for miRNA detection.

Methods	Liner range	LOD	Reference
Colorimetry	50 pM-300 pM	11.3 pM	[2]
Fluorescence	100 fM-1 nM	50 fM	[3]
Electrochemistry	1 pM-25 nM	0.6 pM	[4]
Chemiluminescence	100 fM-10 nM	30 fM	[5]
Eletrochemiluminescence	10 fM-10 pM	10 fM	[6]
Gel electrophoresis	100 fM-1 nM	10 fM	This work

References

1. Li B, Ellington AD, Chen X. Rational, modular adaptation of enzyme-free DNA circuits to multiple detection methods. *Nucleic Acids Res.* 2011; 39: e110.
2. Wen J, Chen J, Zhuang L, Zhou S. Designed diblock hairpin probes for the nonenzymatic and label-free detection of nucleic acid. *Biosens Bioelectron.* 2016; 79: 656-60.
3. Zhang C-H, Tang Y, Sheng Y-Y, Wang H, Wu Z, Jiang J-H. Ultrasensitive detection of microRNAs using catalytic hairpin assembly coupled with enzymatic repairing amplification. *Chem Commun.* 2016; 52: 13584-7.
4. Zhang Y, Yan Y, Chen W, Cheng W, Li S, Ding X, et al. A simple electrochemical biosensor for highly sensitive and specific detection of microRNA based on mismatched catalytic hairpin assembly. *Biosens Bioelectron.* 2015; 68: 343-9.
5. Li D, Cheng W, Li Y, Xu Y, Li X, Yin Y, et al. Catalytic hairpin assembly actuated DNA nanotweezer for logic gate building and sensitive enzyme-free biosensing of microRNAs. *Anal Chem.* 2016; 88: 7500-6.
6. Liao Y, Huang R, Ma Z, Wu Y, Zhou X, Xing D. Target-triggered enzyme-free amplification strategy for sensitive detection of microRNA in tumor cells and tissues. *Anal Chem.* 2014; 86: 4596-604.